

Organic & Biomolecular Chemistry

Accepted Manuscript



This is an *Accepted Manuscript*, which has been through the Royal Society of Chemistry peer review process and has been accepted for publication.

Accepted Manuscripts are published online shortly after acceptance, before technical editing, formatting and proof reading. Using this free service, authors can make their results available to the community, in citable form, before we publish the edited article. We will replace this *Accepted Manuscript* with the edited and formatted *Advance Article* as soon as it is available.

You can find more information about *Accepted Manuscripts* in the [Information for Authors](#).

Please note that technical editing may introduce minor changes to the text and/or graphics, which may alter content. The journal's standard [Terms & Conditions](#) and the [Ethical guidelines](#) still apply. In no event shall the Royal Society of Chemistry be held responsible for any errors or omissions in this *Accepted Manuscript* or any consequences arising from the use of any information it contains.

ARTICLE

Phosphate Modulates Receptor Sulfotyrosine Recognition by the Chemokine Monocyte Chemoattractant Protein-1 (MCP-1/CCL2)

Cite this: DOI: 10.1039/x0xx00000x

Received 00th January 2012,
Accepted 00th January 2012

DOI: 10.1039/x0xx00000x

www.rsc.org/Justin P. Ludeman^a, Mahdieh Nazari-Robati^{a,b}, Brendan L. Wilkinson^c, Cheng Huang^a,
Richard J. Payne^d and Martin J. Stone^{*a}

Tyrosine sulfation is a widespread post-translational modification that mediates the interactions of secreted and membrane-associated proteins in such varied biological processes as peptide hormone action, adhesion, blood coagulation, complement activation and regulation of leukocyte trafficking. Due to the heterogeneous nature of tyrosine sulfation, detailed biochemical and biophysical studies of tyrosine sulfation rely on homogenous, synthetic sulfopeptides. Here we describe the synthesis of a fluorescent sulfopeptide (FL-R2D) derived from the chemokine receptor CCR2 and the application of FL-R2D in direct and competitive fluorescence anisotropy assays that enable the efficient measurement of binding affinities between sulfopeptides and their binding proteins. Using these assays, we have found that the binding of the chemokine monocyte chemoattractant protein-1 (MCP-1) to sulfated peptides derived from the chemokine receptor CCR2 is highly dependent on the assay buffer. In particular, phosphate buffer at close to physiological concentrations competes with the receptor sulfopeptide by binding to the sulfopeptide binding pocket on the chemokine surface. Thus, physiological phosphate may modulate the receptor binding selectivity of chemokines.

Introduction

Protein tyrosine sulfation is an important post-translational modification involved in the modulation of protein-protein interactions in a wide variety of physiological processes. Approximately 50 human proteins are known to be sulfated, the majority of which are peptide hormones and hormone receptors, enzymes, extracellular matrix proteins, blood coagulants and anticoagulants, complement proteins and proteins that function in leukocyte trafficking and adhesion^{1,2}. In particular, most chemokine receptors are tyrosine-sulfated in their N-terminal (extracellular) regions, thus enhancing their interactions with chemokine ligands leading to leukocyte trafficking in inflammatory responses and immune surveillance.

Chemokine receptors and many other tyrosine-sulfated proteins contain multiple potentially sulfated tyrosine residues, commonly occurring in clusters. Efforts to study the effects of tyrosine sulfation upon protein-protein interactions have been hampered by the heterogeneity of sulfation on these multiple residues and the difficulty producing protein samples with defined sulfation patterns. Therefore, we and others have used peptides corresponding to the sulfated regions of proteins to study how tyrosine sulfation functions at the molecular level to modulate protein-protein interactions. These studies have benefited from recent advances in peptide synthesis methodology, allowing access to pure sulfopeptides and sulfoproteins with defined sulfation patterns³⁻⁸. Nuclear Magnetic Resonance (NMR) spectroscopy^{4,9-14} and Electro-

Spray Ionisation Mass Spectrometry (ESI-MS)¹⁵ studies using these sulfopeptides have shown that tyrosine sulfation enhances the affinity and selectivity of chemokines for their receptors and have identified a conserved binding site on chemokines for the tyrosine-sulfated regions of chemokine receptors^{13,14,16,17}. Nevertheless, these studies of sulfotyrosine recognition have been limited due to the large quantities of materials needed and low throughput of NMR studies and the non-equilibrium nature of ESI-MS.

In order to streamline future studies of protein:sulfotyrosine recognition, we have now developed direct and competitive fluorescence anisotropy (FA) plate reader assays for the efficient characterisation of interactions between tyrosine-sulfated peptides and their binding proteins. These assays utilise a fluorescein-conjugated form of a sulfotyrosine-containing peptide corresponding to the N-terminal region of the chemokine receptor CCR2. To optimise the assays, we studied the interaction of an obligate monomeric mutant (P8A) of the chemokine monocyte chemoattractant protein-1 (MCP-1/CCL2) with several differentially-sulfated forms of the CCR2 N-terminal peptide. In the course of assay development we observed that the affinity of MCP-1(P8A) for the fluorescein-conjugated CCR2 sulfopeptide is profoundly sensitive to the assay buffer. In particular we found that the physiological buffer, phosphate, can interact with the sulfotyrosine binding site on MCP-1 thereby inhibiting receptor sulfopeptide binding. These results suggest that physiological phosphate may modulate the receptor binding selectivity of chemokines.

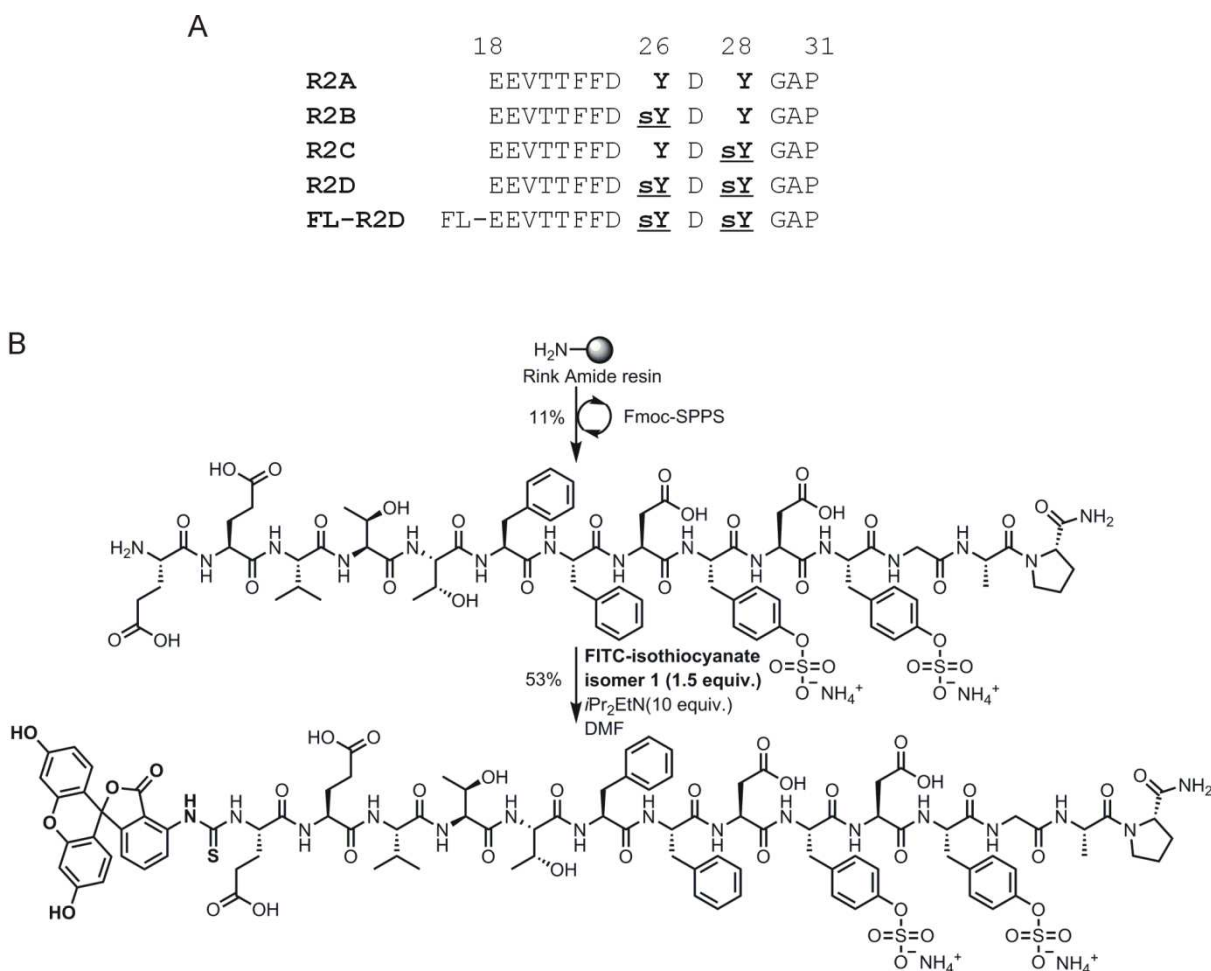


Fig. 1 (Sulfo)peptide sequences and fluorescein labelling. (A) Sequences (one-letter amino acid code) of the CCR2-derived (sulfo)peptides used. Peptides correspond to residues 18-31 of human CCR2. Sulfotyrosine residues are represented as **sY** in bold, underlined font. FL denotes fluorescein linked to the N-terminus of the R2D peptide. (B) Scheme for synthesis of FITC-labelled disulfated peptide FL-R2D.

Results and discussion

Synthesis of Fluorescent Sulfopeptide

We employed a divergent synthesis strategy⁵ to prepare four peptides corresponding to residues 18-31 of CCR2, each containing a different pattern of tyrosine sulfation (Fig. 1A). To facilitate our FA assay, we required access to the doubly-sulfated R2D sulfopeptide containing a conformationally restricted fluorescein moiety, so that the rotational correlation time of the fluorescein moiety would increase substantially upon binding. To circumvent the need for a flexible (not conformationally restricted) alkyl spacer normally required for solid-phase synthesis regimes, we decided to perform the conjugation step in solution using purified, deprotected R2D sulfopeptide (Fig. 1)¹⁸. The purified doubly-sulfated peptide

(R2D) was isolated in 11% overall yield and subsequently reacted with fluorescein isothiocyanate (FITC, isomer 1) in the presence of *N,N*-diisopropylethylamine as a base for 20 h in the dark (Fig. 1B). This led to clean conversion to the N-terminally fluorescein-conjugated sulfopeptide (FL-R2D). Purification by RP-HPLC and repetitive lyophilisation afforded a 53% isolated yield of FL-R2D, which could subsequently be employed in the proposed FA assays.

This relatively straightforward synthetic approach to preparation of FL-R2D was possible, in part, because residues 18-31 of CCR2 do not include any lysine or free cysteine residues whose side chains would also react with FITC. While this was fortuitous for the current study, we note that sulfotyrosine residues commonly occur in highly acidic regions of proteins with few lysine residues, so the same approach could be used to conjugate sulfopeptides from other proteins to

fluorescein or to other biomolecules or functionalities of interest.

Fluorescence Anisotropy Assays for Binding of Proteins to Fluorescent Sulfopeptides

We have utilised the fluorescein-labelled sulfopeptide FL-R2D to develop a FA assay for chemokine binding. In 50 mM MOPS buffer at pH 7 and 25 °C, the FA signal of 10 nM FL-R2D was ~0.02. However, in the presence of increasing concentrations of MCP-1(P8A), a monomeric mutant of the chemokine MCP-1, the FA signal of 10 nM FL-R2D increased monotonically and saturated at a value of ~0.15, indicating that MCP-1(P8A) was binding to FL-R2D (Fig. 2). The binding data fit well to a simple 1:1 binding model (Equation 1) yielding an equilibrium dissociation constant (K_d) of 51.3 ± 2.8 nM. In agreement with the simple binding model, the observed increase in FA signal was consistent with the expected increase in molecular weight for a 1:1 complex.

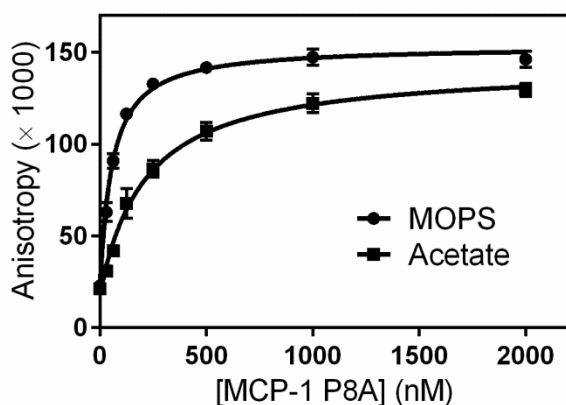


Fig. 2 Direct binding assay for the interaction of MCP-1(P8A) with FL-R2D. Fluorescence anisotropy data (symbols) and fitted curves (solid lines) are shown for experiments performed in 50 mM MOPS buffer, pH 7.0 (●) and 50 mM sodium acetate buffer, pH 7.0 (■), using a constant concentration of 10 nM FL-R2D. Data plotted are the averages of three independent data sets, each recorded in duplicate. Error bars, representing the SEM, are typically smaller than the data points shown.

Having established conditions for reliable observation of the binding between a protein and a fluorescent sulfopeptide, we then sought to develop a robust competitive binding assay whereby the fluorescent sulfopeptide could be competitively displaced from the protein by non-fluorescent (sulfo)peptides with differing sulfation patterns (peptides R2A-D, Fig. 1). For the competitive assay, we employed the same final concentration of FL-R2D (10 nM) used in the direct binding assay and a constant concentration of 100 nM MCP-1(P8A), resulting in approximately 80-90% of the FL-R2D being bound to MCP-1(P8A). Under these conditions (in MOPS buffer) the FA signal was relatively high (~0.12) in the absence of competitive non-fluorescent peptide but decreased monotonically as the concentration of non-fluorescent peptide is increased (Fig. 3), consistent with the expectation of competitive binding. The concentration dependence of FL-R2D displacement by a competing sulfopeptide allows determination of the apparent K_d value for the competitor by non-linear curve fitting (see Experimental).

Fig. 3 shows the competitive displacement data of 5 independent duplicate experiments for (sulfo)peptides R2A-D fitted to the Equation of by Huff et al.¹⁹; the K_d values determined are listed in Table 1. The data show, as expected, that sulfation of tyrosine residues in peptides derived from the N-terminus of CCR2 enhances binding to MCP-1(P8A). Specifically, sulfation of Tyr26 (to give R2B) or Tyr28 (to give R2C) enhances binding 3.8-fold and 1.6-fold, respectively, relative to the non-sulfated peptide (R2A) whereas sulfation of both Tyr residues (to give R2D) gives rise to a 27-fold enhancement in binding affinity compared to the modest affinity (8.6 μ M) of the non-sulfated species. Interestingly, the affinity of the non-fluorescent, doubly-sulfated peptide (R2D) for MCP-1(P8A) was observed to be ~6 times weaker than the affinity of the corresponding fluorescent peptide (FL-R2D) for the same protein, determined in the direct binding assay (see above). This suggests that the fluorescein moiety at the N-terminus of the peptide may interact favourably with the chemokine and/or influence the conformational ensemble of the peptide, thereby strengthening the binding interaction.

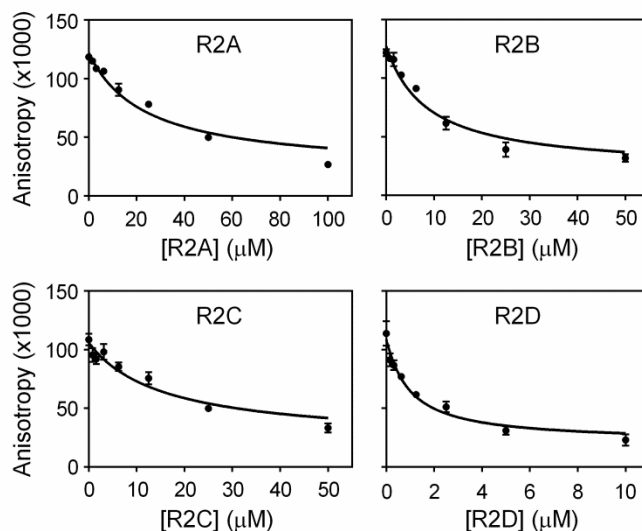


Fig. 3 Competitive displacement of FL-R2D from MCP-1(P8A) by CCR2 (sulfo)peptides. Fluorescence anisotropy data (filled circles) and fitted curves (solid lines) are shown for experiments performed in 50 mM MOPS buffer, pH 7.0 containing constant concentrations of FL-R2D (10 nM) and MCP-1(P8A) (100 nM) and variable concentrations of the indicated CCR2 (sulfo)peptide. The data displayed are the averages of five independent experiments, each recorded in duplicate, with error bars representing the SEM.

Table 1 Affinities of MCP-1 for CCR2-derived (sulfo)peptides determined using the competitive displacement FA assay

Peptide	$K_d \pm \text{Std Err}$ (μ M)	r^2
R2A	8.6 ± 0.8	0.91
R2B	2.3 ± 0.4	0.86
R2C	5.4 ± 0.9	0.70
R2D	0.31 ± 0.06	0.75

Previously we have characterised the binding of peptides R2A-D to MCP-1(P8A) by monitoring chemical shift perturbations in heteronuclear 2D NMR (^{15}N - ^1H HSQC) spectra of ^{15}N -labelled MCP-1(P8A) in the presence of various

peptide concentrations¹⁰. The affinities determined here using the competitive FA assay are compared to the previous NMR-derived affinities in Fig. 4. It is clear that both techniques show the same trend of increasing affinity with increasing peptide sulfation. However, the FA assay yields affinities for peptides R2A, R2B and R2C that are ~46-fold, ~5-fold and ~3-fold higher, respectively, than those determined by NMR. These differences may be influenced by several factors, including: differences in the assay buffer conditions (see below); possible non-specific binding by the non-sulfated peptide (R2A), resulting in divergence from the simple 1:1 binding model; systematic errors involved in the determination of small NMR chemical shift changes; and the impracticality of performing multiple, independent binding measurements by NMR, whereas the FA-derived K_d values and standard errors were obtained by analysis of five independent sets of duplicate binding curves, allowing higher precision and confidence in the K_d values.

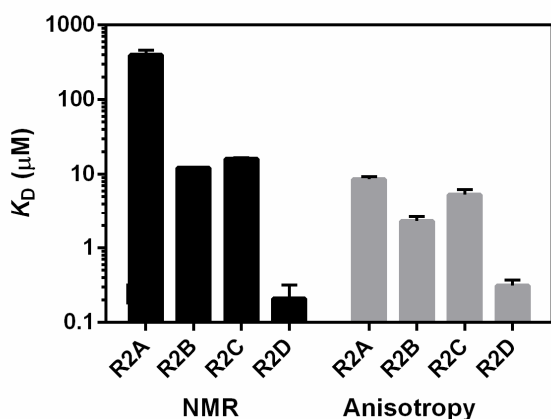


Fig. 4 Comparison of the binding affinities of MCP-1 (P8A) to receptor sulfopeptides (R2A-R2D) measured by NMR (black bars) and competitive fluorescence anisotropy (grey bars).

Influence of Assay Buffer on Binding Affinity

In the course of the above assay development, we noticed that the apparent affinity of MCP-1(P8A) for FL-R2D was substantially lower when the assay was performed in acetate buffer compared to MOPS buffer (Fig. 2). This observation prompted us to systematically screen a series of buffers in the direct binding assay for their influences on: (i) the magnitude of the signal response (change in fluorescence anisotropy, ΔFA); (ii) the quality of the curve fits (r^2 values); (iii) the fitted K_d values; and (iv) the reproducibility and precision of the K_d values determined. Table 2 summarises the data obtained using nine common buffers (all 50 mM, pH 7.0). Among the buffers tested, five buffers (MOPS, Bis-Tris, ACES, acetate and Tris) all gave high quality binding curves ($r^2 > 0.99$ with ΔFA in the range 0.12-0.14). Incidentally, we noticed that data recorded in acetate (a poor buffer at pH 7) were highly sensitive to the incubation time, apparently because evaporation of acetic acid was giving rise to changes in pH and consequent changes in fluorescein fluorescence⁵⁰. With the exception of Tris, all of these five buffers yielded apparent K_d values of ~50-200 nM, but there were reproducible differences in the K_d values determined between the different buffers; Tris buffer substantially weakened the interaction ($K_d = 850 \pm 100$ nM). Moreover, the remaining four buffers (phosphate, PIPES, Bis-Tris Propane and BES) gave poor quality binding data, with relatively high or irreproducible K_d values, low or inconsistent

r^2 values, and small and/or inconsistent changes in anisotropy (Table 2), suggesting that these buffers interfere with the binding interaction.

Table 1 Buffer Dependence of K_d Values Determined for Binding of MCP-1(P8A) to FL-R2D¹

Buffer	$K_d \pm \text{SE}$ (nM)	r^2	$Y_r - Y_i$ (x 1000)
MOPS ²	61 \pm 6	0.990	140
	45 \pm 3	0.996	127
	48 \pm 3	0.997	130
Bis-Tris	78 \pm 7	0.993	113
	75 \pm 12	0.982	128
	67 \pm 11	0.979	122
ACES	177 \pm 18	0.992	162
	203 \pm 10	0.998	134
	183 \pm 16	0.994	134
Acetate	239 \pm 29	0.990	134
	173 \pm 26	0.984	119
	206 \pm 25	0.989	126
Tris	779 \pm 53	0.998	129
	912 \pm 111	0.994	133
	856 \pm 137	0.989	154
Phosphate	1182 \pm 494	0.942	42
	961 \pm 378	0.941	42
	10310 \pm 11860	0.968	239
PIPES	1702 \pm 519	0.976	85
	472 \pm 341	0.775	63
	3655 \pm 1628	0.977	121
Bis-Tris Propane	1408 \pm 1255	0.801	19
	4043 \pm 2182	0.971	50
	873 \pm 409	0.944	25
BES	111 \pm 240	0.206	-1.2
	168 \pm 618	0.090	2.1
	121 \pm 228	0.260	-1.9

¹For each buffer data are shown for each of three independent experiments, each performed in duplicate

²For MOPS, simultaneous fitting of 3 independent duplicate data sets yielded $K_d = 51.3 \pm 2.8$ nM

We have attempted to understand the observed buffer interference effects in light of current structural knowledge on the basis of chemokine:sulfopeptide recognition. Sulfopeptides derived from the N-terminal regions of chemokine receptors bind to a conserved shallow groove formed by the N-loop region and third β -strand ($\beta 3$) of cognate chemokines^{4,9-14,21}. Although the floor of the groove is hydrophobic, the rim of the groove is typically defined by several positively-charged amino acid side chains, which are proposed to interact electrostatically with the sulfotyrosine residues and/or the adjacent acidic residues in the receptor peptides. Any of the buffers used in the current study has the potential to compete with the chemokine:sulfopeptide binding interaction. Negatively-charged functional groups of the buffer could compete by binding to the positively-charged amino acid side chains on the chemokine, whereas positively-charged functional groups of the buffer could compete by binding to the negatively-charged sulfotyrosine or Asp or Glu side chains of the sulfopeptide.

Most of the buffers used herein are zwitterionic so we cannot distinguish *a priori* between these two possible competitive mechanisms. Moreover, there is no obvious simple relationship between the structures or charges of the buffers²² (Tables 2 and S1) and their influences on the binding. For example, MOPS and BES have very similar ionisable groups (sulfonate and tertiary amine) but only BES interferes with the binding interaction, possibly implicating the primary alcohol groups of BES in competitive binding. The other three buffers that substantially interfere with the assay (phosphate, PIPES and Bis-Tris Propane) have the highest numbers of negative charges at pH 7 among the nine buffers tested (Table S1) suggesting that the primary mechanism of interference may be non-specific binding to basic groups on the chemokine. However, PIPES also contains two positively-charged (tertiary amine) groups positioned in a manner that could enable binding to sulfonate or carboxylate groups of the receptor sulfopeptide. Similarly, the weaker binding in Tris buffer compared to, for example, Bis-Tris may be attributable to screening of negatively-charged groups in the sulfopeptide by the primary amine moiety in the Tris buffer. We emphasise that the buffer concentrations used in these experiments are 5,000,000-fold higher than the concentration of FL-R2D (50 mM versus 10 nM). Thus, even for buffers that substantially disrupt binding, the buffers are likely to interact with the chemokines at much lower affinities than the chemokine:sulfopeptide interaction of interest.

Phosphate Competes with Receptor Sulfopeptide for Binding to Chemokine MCP-1

Among the buffers investigated herein, the influence of phosphate was of particular interest due to its physiological relevance. Fig. 5A shows the effects of 12.5, 25, 50 and 100 mM phosphate in 50 mM MOPS buffer (pH 7.0) on the strength of binding between MCP-1(P8A) and FL-R2D; the apparent K_d values are plotted in Fig. 5B. Clearly phosphate is inhibiting sulfopeptide binding to MCP-1(P8A) in a concentration-dependent manner. To investigate the hypothesis that phosphate ions were competing with the sulfotyrosine residues for binding to the basic groove on the surface of the chemokine, we recorded 2D ^{15}N - ^1H correlation (HSQC) NMR experiments on ^{15}N -enriched MCP-1(P8A) in the presence of various concentrations of sodium phosphate or, as a control, sodium chloride. Sodium phosphate induced concentration-dependent changes in weighted backbone amide chemical shifts exceeding 0.02 ppm for 10 residues of MCP-1(P8A), whereas sodium chloride had a smaller influence on backbone amide chemical shifts (Figs. 5C, 5D and S1). The majority of residues whose NMR signals were sensitive to phosphate are clustered in two patches on the protein structure (Fig. 5D). Six of these residues (R24, L25, I46, K49, E50 and I51) are in or adjacent to the previously identified binding groove for CCR2 sulfopeptides (Fig. 5D, left), strongly supporting the proposal that phosphate ions complete with peptide sulfotyrosine residues for binding to this groove. The second, smaller cluster of residues (V60, D65 and H66) is on the opposite face of MCP-1 from the sulfopeptide binding site (Fig. 5D, right) and therefore unlikely to substantially influence binding. Considering that phosphate occurs at concentrations of ~1-1.5 mM in human serum²³, we suggest that phosphate may compete effectively for receptor binding to weak, non-cognate chemokines while still allowing binding by higher affinity, cognate chemokines. In this way, physiological phosphate could help to regulate the selectivity of chemokine:receptor interactions.

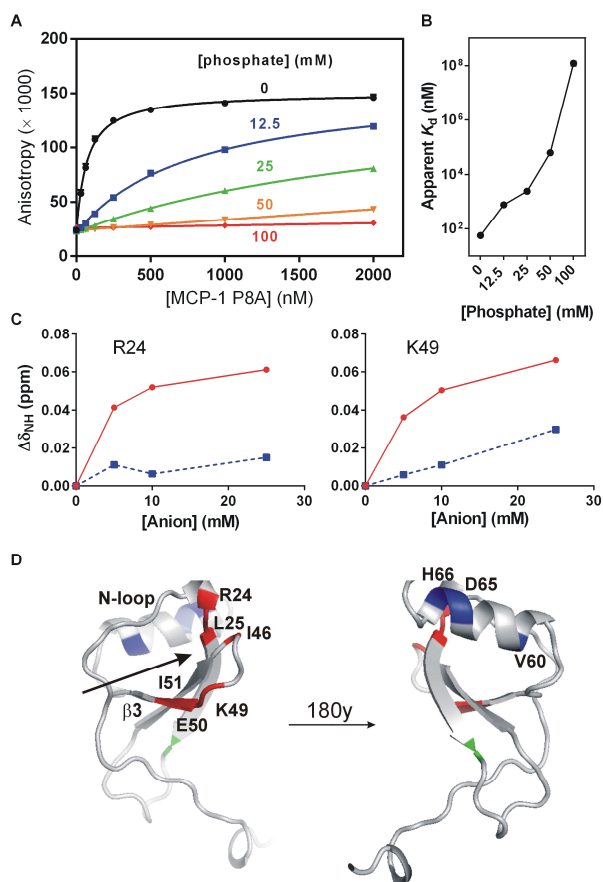


Fig. 5 Phosphate competes with FL-R2D for binding to MCP-1(P8A). (A) Binding curves recorded in 50 mM MOPS buffer containing 0 (black), 12.5 (blue), 25 (green), 50 (orange) and 100 mM (red) sodium phosphate buffer (pH 7.0). Data plotted are the averages of three independent data sets, each recorded in duplicate. Error bars, representing the SEM, are typically smaller than the data points shown. (B) Graph showing the increase in apparent K_d as a function of phosphate concentration. Error bars, representing the SEM from three independent experiments, are smaller than the data symbols. (C) Chemical shift changes for two representative NH groups (R24 and K49) as a function of sodium phosphate (red) or sodium chloride (blue) concentration. Data for additional residues are in Supplementary Material (Fig. S1). (D) The monomer structure of MCP-1 (PDB code: 1DOM), shown as light grey ribbons with residues influenced by phosphate ($\Delta\delta_{\text{NH}} \geq 0.02$ ppm in 25 mM phosphate) highlighted in colour (N-loop and $\beta 3$ -strand, red; C-terminal α -helix, blue; I31, green) and labelled. The two views are related by a 180° rotation around the vertical (y) axis. The location of the sulfopeptide binding groove is indicated by an arrow on the left-hand view.

Experimental

Materials. The buffers N-(2-acetamido)-2-aminoethanesulfonic acid (ACES), sodium acetate, N,N-bis(2-hydroxyethyl)-2-aminoethanesulfonic acid (BES), 2,2-bis(hydroxymethyl)-2,2',2''-nitilotriethanol (Bis-Tris), 1,3-bis[tris(hydroxymethyl)methylamino]propane (Bis-Tris Propane), 3-(N-morpholino) propanesulfonic acid (MOPS), piperazine-1,4-bis(2-ethanesulfonic acid) (PIPES), and tris(hydroxymethyl)aminomethane (Tris) were obtained from Sigma-Aldrich. Sodium dihydrogen phosphate (NaH_2PO_4) and

disodium hydrogen phosphate (Na_2HPO_4) salts were obtained from Merck. All buffers were prepared fresh, sterile filtered and degassed, and contained 0.02% w/v NaN_3 as preservative. Solvents and chemicals, including Fmoc-protected amino acids, DMF, coupling reagents and activator bases were purchased from Mimotopes, Sigma Aldrich and Merck, and used without further purification; Fmoc-protected, side chain neopentyl-protected sulfotyrosine [Fmoc-Tyr(SO_3np)-OH] was synthesised as described^{5,11}. Anhydrous dichloromethane (DCM) was distilled from CaH_2 and stored on activated 4 Å sieves. Fmoc-strategy solid phase peptide synthesis (Fmoc-SPPS) was performed manually in Torvic fritted syringes..

Divergent Solid-Phase Peptide Synthesis (SPPS) of Sulfopeptides R2A-D. Rink amide resin (200 μmol) was initially loaded with Fmoc-Pro-OH. The peptide was elongated (in C- to N-terminal direction) up to the first sulfotyrosine residue (Y28) using iterative coupling, capping (acetylation) and Fmoc-deprotection protocols (Fmoc-SPPS). The resin was then split into 4 equal batches (50 μmol each) and iterative Fmoc-SPPS was performed on a 50 μmol scale to generate the differentially sulfated peptides, which were then cleaved from the resin. Detailed procedures for the resin loading, capping, Fmoc-deprotection, coupling and cleavage from the resin are presented in the Supplementary Material. Peptides containing sulfated Tyr residues were neopentyl (nP) deprotected as follows. A suspension of the crude sulfopeptide in Milli-Q water (1 mg/mL) was prepared and sodium azide (50 equiv.) was added in a single portion. The mixture was stirred at 70 °C for 16 h. The mixture was cooled and directly purified by preparative RP-HPLC to give pure sulfopeptides R2B-D. Isolated yields of (sulfo)peptides after HPLC purification were 11-26% based on the original 50 μmol resin loading; additional details are presented in the Supplementary Material.

Preparation of Fluorescent Sulfopeptide Fluorescein-R2D (FL-R2D). A solution of purified sulfopeptide R2D (5 mg, 3 μmol) was prepared in dry DMF (200 μL) under argon. *N,N*-diisopropylethylamine (5.2 μL , 30 μmol , 10 equiv.) was added followed by fluorescein isothiocyanate (isomer 1) (1.8 mg, 4.5 μmol , 1.5 equiv.). The bright yellow solution was agitated in the dark for 20 h. The solution was quenched by the addition of 0.1 M ammonium acetate (1 mL) and immediately purified by semi-preparative RP-HPLC. The material was freeze-dried multiple times from Milli-Q water until a consistent weight was achieved. Fluorescent sulfopeptide FL-R2D was isolated as a yellow solid (3.6 mg, 1.6 μmol , 53%) and characterised as for the other (sulfo)peptides (see above and Supplementary Material).

Purification and Characterisation of (Sulfo)peptides R2A-D and FL-R2D. All peptides were purified by preparative RP-HPLC performed using a Waters 600 Multisolvant Delivery System and Waters 500 pump with 2996 photodiode array detector or Waters 490E Programmable wavelength detector. (Sulfo)peptides R2A-D and FL-R2D were purified on a Waters

Xbridge BEH300 5 μm preparative column (C-18) operating at a flow rate of 7 ml min⁻¹ using a linear gradient of 0.1 M ammonium acetate in water (Solvent A) and acetonitrile (Solvent B). Pure fractions containing product were collected and lyophilized multiple times from Milli-Q water until a consistent weight was achieved.

Purified peptides were characterised by analytical RP-HPLC and LC-MS. Analytical RP-HPLC was performed on a Waters System 2695 separations module with an Alliance series column heater at 30 °C and 2996 photodiode array detector. (Sulfo)peptides R2A-D and FL-R2D were analysed using a Waters Xbridge BEH300 5 μm , 2.1 x 150 mm column (C-18) at a flow rate of 0.2 ml min⁻¹ using a linear gradient of 0.1 M ammonium acetate in water (Solvent A) and acetonitrile (Solvent B). LC-MS was performed on a Shimadzu LC-MS 2020 instrument consisting of a LC-M20A pump, a SPD-M20A Photodiode array detector coupled to a Shimadzu 2020 mass spectrometer (ESI) operating in negative ion mode for all sulfopeptides. Separations were performed on a Waters Sunfire 5 μm , 2.1 x 150 mm column (C18) or a Waters Symmetry 300 5 μm , 2.1 x 150 mm (C4) column, operating at a flow rate of 0.2 mL min⁻¹ using a linear gradient of 0.1% formic acid in water and 0.1% formic acid in acetonitrile as mobile phase. HPLC traces and LC-MS data for all (sulfo)peptides are presented in the Supplementary Material. Sulfopeptide concentrations of FA assay stocks were determined by UV spectrophotometry and RP-HPLC as previously described¹¹.

Protein Production and Characterisation. MCP-1(P8A) was expressed and purified as described previously⁹. Briefly, *E. coli* inclusion bodies containing overexpressed N-terminally His₆-tagged MCP-1(P8A) were washed, denatured and purified by immobilised metal affinity chromatography (IMAC) using Ni-NTA-agarose (Qiagen). Purified denatured inclusion bodies were refolded by rapid dilution into 20 mM Tris, pH 8.0, 400 mM NaCl, 2 mM reduced glutathione and 0.5 mM oxidised glutathione. Refolded protein was concentrated and further purified by IMAC using a HisTrap column (GE Healthcare) prior to thrombin cleavage. Cleaved protein was separated from the His₆-tag and uncleaved protein by IMAC and polished by cation exchange chromatography using a HiTrap SP column (GE Healthcare). MCP-1(P8A) was shown to be monomeric and of high purity by silver stained SDS-PAGE and analytical size exclusion chromatography using a calibrated Yarra SEC 2000 column (Phenomenex). Protein stocks were frozen in 20 mM sodium acetate, pH 7.0 and were defrosted and diluted into the requisite buffer(s) immediately prior to use.

Fluorescence Anisotropy Binding Assays. All FA assays were performed at 25 °C using Greiner non-binding, black, flat-bottomed, 96-well microplates (catalogue no. 655900) and a BMG Labtech PHERAstar FS plate reader equipped with a fluorescence polarisation module with dedicated excitation and emission wavelengths of 520 and 585 nm, respectively.

The direct binding assay was performed using a constant concentration of FL-R2D (final concentration 10 nM) and

serially 2-fold diluted MCP-1(P8A) ranging in concentration from 2.0 μM to 31.3 nM, in 50 mM of pH 7.0 buffer (see Table 2) and a final volume of 200 μL in each well. Duplicate assays were performed three times independently and the average data plotted and fitted by non-linear regression analysis using GraphPad Prism v.6.0 software to a simple equilibrium 1:1 binding model, described by the equation:

$$Y = \frac{Y_i + (Y_f - Y_i) \times (1/2P_f) [(P_f + L_f + K_d) - \sqrt{(P_f + L_f + K_d)^2 - 4P_f L_f}]}{2} \quad [\text{Equation 1}]$$

in which: Y is the observed anisotropy signal; Y_i and Y_f are the fitted initial and final anisotropy signals, respectively; P_f is the total concentration of FL-R2D; L_f is the total concentration of MCP-1(P8A); and K_d is the fitted equilibrium dissociation constant. The effects of phosphate on binding of MCP-1(P8A) to FL-R2D were determined by 3 independent duplicate experiments using serially 2-fold diluted phosphate buffer ranging in concentration from 12.5 – 100 mM, in 50 mM MOPS (pH 7.0).

The competitive binding assay was performed using constant final concentrations of 10 nM FL-R2D and 100 nM MCP-1(P8A) with serially 2-fold diluted non-fluorescent (sulfo)peptides R2A-R2D, with highest concentrations of 200 μM (for R2A), 50 μM (for R2B and R2C) or 10 μM (for R2D), consistent with the expected decreases in K_d with increasing degree of sulfation. All competitive binding assays were performed in 50 mM MOPS, pH 7.0 with final sample volumes of 200 μL in each well. Duplicate assays were performed five times independently and the average data fitted by non-linear regression analysis using GraphPad Prism v.6.0 software to the equation for a 1:1 competitive displacement curve described by Huff et al.¹⁹, in which: the independent variable is the concentration of non-fluorescent (sulfo)peptide; the dependent variable is the observed anisotropy signal; fixed input parameters are the total concentrations of FL-R2D and MCP-1(P8A), the final anisotropy signal, which is the anisotropy of free FL-R2D, and the K_d for 1:1 binding between FL-R2D and MCP-1(P8A), determined using the direct binding assay; and fitted parameters are the initial anisotropy signal and the K_d for 1:1 binding of the non-fluorescent (sulfo)peptide to MCP-1(P8A).

NMR Mapping of Phosphate Binding to MCP-1(P8A). Two-dimensional ^{15}N -HSQC spectra were recorded at 25 $^\circ\text{C}$ on a Bruker 600 MHz spectrometer equipped with a triple-resonance cryogenic probe. ^1H chemical shifts were referenced to DSS (0 ppm) and ^{15}N chemical shifts were indirectly referenced to ammonia as described²⁴. Samples contained 50 mM uniformly ^{15}N -labelled MCP-1(P8A) in 20 mM deuterated sodium acetate, 0.02% NaN_3 , 5% D_2O (pH 7.0) in addition to either: no added salts; 5, 10 or 25 mM sodium phosphate; or 5, 10 or 25 mM sodium chloride. The final pH of all samples was adjusted to 7.0. Spectra were analysed using Sparky (T. D. Goddard and D.

G. Kneller, University of California, San Francisco, CA) and graphical analysis was performed using GraphPad Prism v.6.0. The weight change in amide chemical shift ($\Delta\delta_{\text{NH}}$) for each residue was calculated from the changes in ^1H and ^{15}N chemical shifts ($\Delta\delta_{\text{H}}$ and $\Delta\delta_{\text{N}}$, respectively) using the formula: $\Delta\delta_{\text{NH}} = |\Delta\delta_{\text{H}}| + 0.2 |\Delta\delta_{\text{N}}|$.

Conclusions

We have established robust direct and competitive fluorescence anisotropy binding assays for determining the affinities of soluble proteins for peptides containing sulfotyrosine residues. These assays offer substantial practical advantages over previous approaches; they are efficient, reliable and economical. Using these assays, we have found that the affinity of the chemokine MCP-1 for a receptor-derived sulfopeptide is profoundly sensitive to the assay buffer. In particular, phosphate competes with the receptor sulfopeptide by interacting with the sulfopeptide binding site on the surface of the chemokine, apparently mimicking the interactions of the tyrosine sulfate moieties. Based on these results, we propose that physiological phosphate buffer is a previously unrecognised factor that modulates the affinities and selectivities of sulfated chemokine receptors for their cognate chemokines. Considering the similarity between sulfate moieties and phosphate ions, it is possible that this regulatory mechanism also applies to the interactions of other sulfotyrosine-containing proteins.

Acknowledgements

This work was supported by Australian Research Council grants DP1094884 and DP130101984 (to RJP and MJS) and LE0989504 (to MJS), ARC Future Fellowship FT130100150 (to RJP) and ARC DECRA fellowship DE130101673 (to BLW).

Notes and references

- ^a Department of Biochemistry and Molecular Biology, Monash University, Clayton, VIC 3800, Australia. E-Mail: martin.stone@monash.edu.
- ^b Department of Biochemistry, Kerman University of Medical Sciences, Kerman, Iran.
- ^c School of Chemistry, Monash University, Clayton, VIC 3800, Australia.
- ^d School of Chemistry, Building F11, The University of Sydney, NSW 2006, Australia.
- †Electronic Supplementary Information (ESI) available: Detailed procedures for peptide synthesis and characterisation; peptide analytical data; table of buffer structures and charges; figure showing MCP-1(P8A) chemical shift changes upon addition of phosphate or chloride.

- M. J. Stone, S. Chuang, X. Hou, M. Shoham and J. Z. Zhu, *N. Biotechnol.*, 2009, 25, 299-317.
- M. Szpakowska, V. Fievez, K. Arumugan, N. van Nuland, J. C. Schmit and A. Chevigne, *Biochem. Pharmacol.*, 2012, 84, 1366-1380.
- L. S. Simpson and T. S. Widlanski, *J. Am. Chem. Soc.*, 2006, 128, 1605-1610.
- L. S. Simpson, J. Z. Zhu, T. S. Widlanski and M. J. Stone, *Chem. Biol.*, 2009, 16, 153-161.

5. D. Taleski, S. J. Butler, M. J. Stone and R. J. Payne, *Chem. Asian J.*, 2011, 6, 1316-1320.
6. Y. S. Y. Hsieh, D. Taleski, B. L. Wilkinson, L. C. Wijeyewickrema, T. E. Adams, R. N. Pike and R. J. Payne, *Chem. Commun.*, 2012, 48, 1547-1549.
7. Y. S. Y. Hsieh, L. C. Wijeyewickrema, B. L. Wilkinson, R. N. Pike and R. J. Payne, *Angew. Chem. Int. Edit.*, 2014, 53, 3947-3951.
8. X. Liu, L. R. Malins, M. Roche, J. Sterjovski, R. Duncan, M. L. Garcia, N. C. Barnes, D. A. Anderson, M. J. Stone, P. R. Gorry and R. J. Payne, in *ACS Chem. Biol.*, 2014, 9, 2074-2081.
9. J. H. Tan, M. Canals, J. P. Ludeman, J. Wedderburn, C. Boston, S. J. Butler, A. M. Carrick, T. R. Parody, D. Taleski, A. Christopoulos, R. J. Payne and M. J. Stone, *J. Biol. Chem.*, 2012, 287, 14692-14702.
10. J. H. Tan, J. P. Ludeman, J. Wedderburn, M. Canals, P. Hall, S. J. Butler, D. Taleski, A. Christopoulos, M. J. Hickey, R. J. Payne and M. J. Stone, *J. Biol. Chem.*, 2013, 288, 10024-10034.
11. J. Z. Zhu, C. J. Millard, J. P. Ludeman, L. S. Simpson, D. J. Clayton, R. J. Payne, T. S. Widlanski and M. J. Stone, *Biochemistry*, 2011, 50, 1524-1534.
12. L. Duma, D. Haussinger, M. Rogowski, P. Lusso and S. Grzesiek, *J. Mol. Biol.*, 2007, 365, 1063-1075.
13. C. T. Veldkamp, C. Seibert, F. C. Peterson, T. P. Sakmar and B. F. Volkman, *J. Mol. Biol.*, 2006, 359, 1400-1409.
14. C. T. Veldkamp, C. Seibert, F. C. Peterson, N. B. De la Cruz, J. C. Haugner, 3rd, H. Basnet, T. P. Sakmar and B. F. Volkman, *Sci. Signal.*, 2008, 1, ra4.
15. C. H. Jen and J. A. Leary, *Anal. Biochem.*, 2010, 407, 134-140.
16. J. P. Ludeman and M. J. Stone, *Brit. J. Pharmacol.*, 2014, 171, 1167-1179.
17. C. J. Millard, J. P. Ludeman, M. Canals, J. L. Bridgford, M. G. Hinds, D. J. Clayton, A. Christopoulos, R. J. Payne and M. J. Stone, *Structure*, 2014, in press.
18. M. Jullian, A. Hernandez, A. Maurras, K. Puget, M. Amblard, J. Martinez, G. Subra, *Tetrahedr. Lett.* 2009, 50, 260-263.
19. S. Huff, Y. V. Matsuka, M. J. McGavin and K. C. Ingham, *The J. Biol. Chem.*, 1994, 269, 15563-15570.
20. M. M. Martin and L. Lindqvist, *J. Lumin.*, 1975, 10, 381-390.
21. E. Schnur, N. Kessler, Y. Zherdev, E. Noah, T. Scherf, F. X. Ding, S. Rabinovich, B. Arshava, V. Kurbatska, A. Leonciaks, A. Tsimanis, O. Rosen, F. Naider and J. Anglister, *FEBS J.*, 2013, 280, 2068-2084.
22. R. N. Goldberg, N. Kishore and R. M. Lennen, *J. Phys. Chem. Ref. Data*, 2002, 31, 231-370.
23. V. K. Bansal, in *Clinical Methods: The History, Physical, and Laboratory Examinations*, ed. H. K. Walker, Hall, W.D., Hurst, J.W., Butterworths, Boston, 3 edn., 1990.
24. D. S. Wishart, C. G. Bigam, J. Yao, F. Abildgaard, H. J. Dyson, E. Oldfield, J. L. Markley and B. D. Sykes, *J. Biomol. NMR*, 1995, 6, 135-140.